SEARCH FOR MARINE ICE SHEETS IN PLEISTOCENE BERINGIA

T.J. Hughes (Department of Geological Sciences and Institute for Quaternary Studies University of Maine Orono, Maine 04469)

ABSTRACT

Marine ice sheets that form when sea ice thickens and grounds on shallow polar continental shelves have stable seaward margins on the continental slope where the bed slopes sharply downward seaward, and stable landward margins when the snowline exceeds a critical upward slope landward, according to glaciological theory. However, seaward margins become unstable when isostatic depression beneath the ice sheet produces a bed that slopes upward seaward, and landward margins become unstable when the Milankovitch insolation cycle or other climatic forcing produces a snowline slope less than the critical angle. These instabilities are accentuated if the marine ice sheet becomes thick enough to allow its frozen bed to become thawed, so that ice-cemented marine sediments become a slurry that provides little basal traction to restrain gravitational collapse of the ice sheet. These unstable conditions replace the stable conditions when a marine ice sheet has existed for about 10,000 years on the broad arctic continental shelf of western and central Beringia. As a result of these instabilities, a marine ice sheet grounded in the East Siberian Sea and the Chukchi Sea would surge into the Chukchi Foreland to the north and into the Bering Sea to the south. This could halt human migrations on the "land bridge" across central Beringia. Vertical collapse and areal expansion permit isostatic rebound and refreezing of the bed, so the ice sheet can retreat and thicken as the snowline slope again steepens. The cycle can then repeat. These results are simulated by a computer model. Field studies are proposed to determine if a marine ice sheet existed and had this behavior. The tests include coring into the Pleistocene sediments on the arctic continental shelf and searching for glacial geological evidence, including marine deposits, on the islands and coastal lowlands of arctic Siberia.

INTRODUCTION

Pleistocene Beringia is the landmass extending from the Lena River in Russia to the Mackenzie River in Canada. It is generally believed to have been a land bridge from Siberia to Alaska during Quaternary glaciations, when Northwestern Hemisphere ice sheets lowered sea level enough to expose central Beringia, shown in Figure 1. After the last Pleistocene glaciation, rising Holocene sea level flooded central Beringia, which is now mostly covered by the Chukchi and Bering Seas. According to the prevailing view, only highland glaciers developed in central Beringia during the Pleistocene glaciations, and highland glaciation rarely extended onto present-day coastal plains, especially in Alaska (Hopkins, 1972, 1982; Biryukov and others, 1988; Hamilton, 1991). The plains of central Beringia are believed to have been part of a vast grassy steppe that supported large grazing mammals during the last Pleistocene glaciation (Guthrie, 1990).

This view of Pleistocene Beringia is incompatible with the fact that aboriginal people of southeast Asia were able to cross a deep ocean strait and populate Australia 80,000 years ago, but aboriginal people of northeast Asia were unable to cross a broad grassy plain teeming with game and occupy North America in any substantial numbers until 12,000 years ago. If highland glaciation was generally restricted in Pleistocene Beringia, and was therefore unable to block the land bridge from Siberia to Alaska, perhaps marine glaciation that transgressed central Beringia from the Chukchi Sea to the Bering Sea was able to provide a barrier to human migration for most of the last 80,000 years (Hughes and Hughes, 1994). Marine ice sheets are ice sheets grounded below sea level, such that their margins either become afloat or calve in deep water. The only present-day marine ice sheet is the West Antarctic Ice Sheet, which is grounded to an average depth of 500 m below sea level on the broad continental shelf of Antarctica in the Western Hemisphere (van der Veen and Oerlemans, 1987). This paper examines conditions for inception, advance, retreat, and collapse of Pleistocene marine ice sheets on the broad Arctic continental shelf of Eurasia, and the implications for Pleistocene Beringia.

NUCLEATING MARINE ICE SHEETS

It is postulated that marine ice sheets, including the West Antarctic Ice Sheet, form when sea ice thickens and grounds on polar continental shelves (Wexler, 1961; Denton and Hughes, 1981; Hughes, 1987). The basic equation for sea-ice thickening is (Crary, 1960):

$$\frac{dh_I}{dt} = a + \frac{(K/h_I)\Delta T - Q_H}{\rho_I H_M} = \frac{C_1}{h_I} + C_2 \tag{1}$$

where h_I is ice thickness, t is time, a is the top surface accumulation rate (positive) or ablation rate (negative) of ice, K is the thermal conductivity of ice, ΔT is the mean annual temperature increase form the top to the bottom surface of sea ice, Q_H is the heat flux supplied to the bottom surface by water currents, ρ_I is ice density, H_M is the latent heat of melting, and:

$$C_1 = K\Delta T / \rho_I H_M \tag{2}$$

$$C_2 = a - Q_H / \rho_I H_M \tag{3}$$

When a, Q_H, and ΔT do not vary over time, C_1 and C_2 are constants and Equation (1) can be integrated to give the variation of sea ice thickness with time:

$$t = \frac{h_I}{C_1} - \left(\frac{C_2}{C_1^2}\right) ln\left(1 + \frac{C_1 h_I}{C_2}\right) \tag{4}$$

Fig. 1. Beringian location map.
Bathymetry contours are from the 200 m isobath to present-day sea level. Identified by letters are the Gulf of Anadyr (A), Kotzebue Sound (K), Norton Sound (N), Bristol Bay (B), Bristol Trough (BR), Bering Trough (BE), Herald Canyon (H), Saint Lawrence Island (SL), Wrangel Island (W), and the New Siberian Islands (NSI).
From Ackerman, Figure 2 (1988).

Figure 2 is a plot of h_I versus t for values of and Q_H, listed in Table I when ΔT = 15°C. For example, if Q_H = 0 and a = 0.1 m/a, sea ice would ground in water less than 100 m deep in less than 500 years. This would include vast areas of the Eurasian Arctic continental shelf from Spitzbergen to Alaska.

The major water currents now supplying heat to the bottom surface of sea ice on the Eurasian Arctic continental shelf of Eurasia are the large Siberian rivers. When sea ice thickens and grounds to a depth of 10 m or more on the Siberian Arctic continental shelf, cracks opened by winds and tides will not fracture the full thickness of sea ice because hydrostatic compression of basal ice will exceed tensile stresses that open the cracks (Nye, 1957). Under these conditions, water discharged by the Siberian rivers will pond on the top surface of sea ice and freeze during the following winter. This frozen water layer is then added to winter snowfall to augment a in Equation (1), in which $Q_H \approx 0$ because Siberian rivers no longer deliver heat to the bottom surface of sea ice.

Sea ice grounded on the Siberian Arctic continental shelf eventually thickens to an elevation that dams the Siberian rivers, so the rivers become ice-dammed lakes that expand across the Arctic coastal plain of Siberia. These lakes will be shallow, so they can freeze to the bottom during Siberian winters to become vast "icings" similar to those observed today in the Moma Depression of the Moma River, which joins the Indigirka River in

northeast Siberia. In the Moma Depression, tributaries of the upper Moma River are frozen to their beds, so mountain streams must discharge summer meltwater over the ice surface, and this meltwater freezes in the winter to expand the areal extent of the icings.

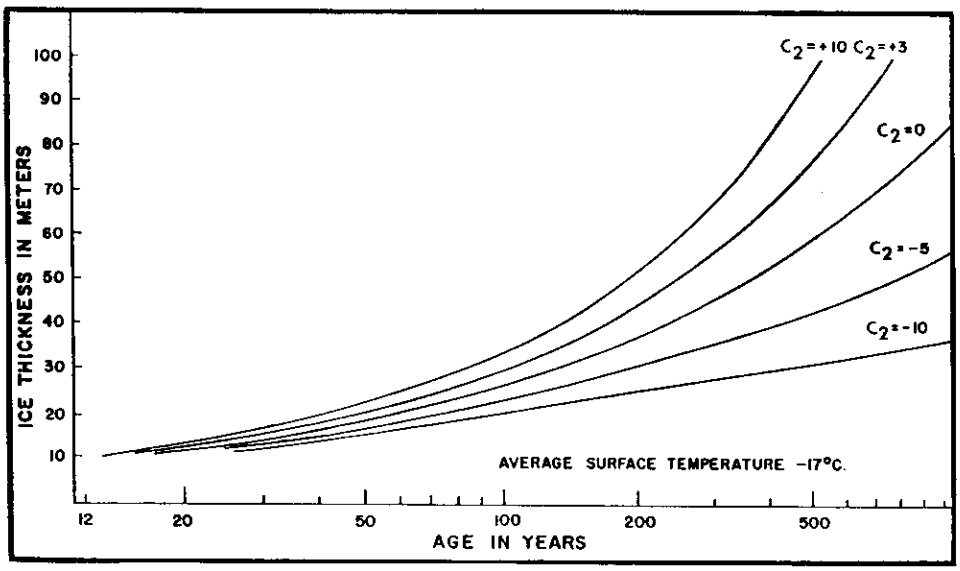

Fig. 2. Rates of thickening for sea ice.
Thickness of sea ice at various times plotted from Equation (3) for an average surface temperature of -17°C and various combinations of surface accumulation rates and basal heating rates listed in Table 1 and added to produce coefficient C_2 in Equation (4).
From Crary (1960).

The combined areal extent of sea ice grounded on the Siberian Arctic continental shelf and lake ice grounded on the Siberian Arctic coastal plain constitutes the nucleus of marine ice sheets in Arctic Eurasia. This ice grounds in situ on a frozen bed, so the bed is preserved in its state at the time of grounding. Snow accumulating on the ice surface during winter cannot drain from the flat surface when it melts during the summer, so the meltwater will pond and refreeze during the following winter. Therefore the entire area of grounded sea and lake ice is an accumulation zone, so it will become domed as it thickens. Eventually, the ice surface along the edge of these ice domes will become steep enough to allow drainage of summer meltwater in excess of that which soaks into the winter snowpack and refreezes. Doming will also allow the grounded ice to creep in downslope directions. Creep converts the grounded ice into an ice sheet thick enough to spread under its own weight. This begins the advance stage of a marine ice sheet.

ADVANCING MARINE ICE SHEETS

Marine ice sheets will advance to the edge of the continental shelf and onto the coastal plain of Siberia over a bed that initially is frozen, because permafrost blankets these offshore and onshore regions today (Gavrilova, 1981; Bigl, 1984). Ice advance will be resisted by traction provided by the frozen bed.

Basal traction is represented by basal shear stress τ_0 defined as the product of ice density ρ_I, gravitational acceleration g_z, ice thickness h_I, and ice surface slope α for a coordinate system in which x is horizontal along flowlines and z is vertical:

$$\tau_0 = \rho_I g_z h_I \alpha \tag{4a}$$

Taking x positive from the ice margin to the ice divide, ice elevations along surface flowlines of an ice sheet can be computed from Equation (4) by writing it in the following numerical form:

$$h_{i+1} = h_i + \left(\frac{\tau_0}{h_I}\right)_i \frac{\Delta X}{\rho_I g_z} = h_i + \left(\frac{\tau_0}{h - h_R}\right)_i \frac{\Delta X}{\rho_I g_z} \tag{5}$$

where $\alpha = \Delta h/\Delta x$, $\Delta h = h_{i+1} - h_i$ is the change in ice elevation in constant step length Δx along a flowline of length L divided into $L/\Delta x$ equal steps from the ice margin to the ice divide, integer i denotes the step, bed

elevation $h_R = h - h_I$, and $[\tau_0/(h - h_R)]_i$ must be specified at each step. Glacioisostatic depression of the bed lowers the surface from elevation h to elevation h^* above the bed at the ice-sheet margin, and lowers the bed from h_R to h_R^* above or below the bed at the ice-sheet margin. The bed at the ice-sheet margin is assumed to be unaffected by glacioisostasy. Taking r as the ratio of the lowered surface to the lowered bed:

$$r = \frac{h^* - h_R}{h_R - h_R^*} \tag{6}$$

it can be shown that Equation (5) becomes (Hughes, 1985):

$$h_{i+1}{}^* = h_i{}^* + \left(\frac{\tau_0}{(1+r)\,h^* - (1+r)^{1/2} h_R} \right)_i \frac{\Delta X}{\rho_I g_z} \tag{7}$$

and that h_R^* is linked to h_R for present-day topography or bathymetry by the expression:

$$h_R{}^* = (1+r)^{1/2} h_R - r h^* \tag{8}$$

If ρ_I = 917 kg/m^3 for ice density and ρ_R = 3600 kg/m^3 for the mean density of Earth's mantle, isostatic equilibrium requires that:

$$r = r_0 = \frac{\rho_I}{\rho_R - \rho_I} \approx \frac{1}{3} \tag{9}$$

Taking t_0 as the time constant for glacioisostatic compensation beneath an ice sheet, the value of r for an ice sheet advancing over time t is:

$$r = r_0 [1 - exp(-t/t_0)] \tag{10}$$

and the value of r for an ice sheet retreating over time t is:

$$r = r_a exp(-t/t_0) \tag{11}$$

where r_a is the value of r in Equation (10) when advance ends and retreat begins.

Equation (7) is an initial-value finite-difference recursive formula. The initial value of ice thickness is $h_I = h_0$ for i = 0. For a marine ice margin, the condition for ice just becoming afloat in water of density ρ_w and depth h_w is:

$$h_0 = h_w (\rho_w / \rho_I) \tag{12}$$

For a calving ice wall at a lacustrine or tidewater ice margin h0 is less than that given by Equation (12), unless the ice wall is nearly afloat. For terrestrial ice margins where the bed is frozen and flat, τ_0 and h_R are constant so that Equation (4) can be integrated by setting $\alpha = dh_I/dx$. Integrating for $h_I = h_0$ for i = 0 and $x \ll \Delta x$ gives:

$$h_0 = (2\tau_0 x/\rho_I g_z)^{1/2} \tag{13}$$

The finite difference in Equation (7) is Δx. The recursive feature of Equation (7) is that, once the initial h_i is specified by either Equation (12) or Equation (13), h_{i+1} for the next Δx step is calculated readily and becomes h_i for calculating h_{i+1} in the following step, a process that recurs along a flowline of length L until step $i = L/\Delta x$ at the ice divide. Modified Euler or Runge-Kutta solutions of Equation (7) are available to reduce the dependence of h on the length Δx of steps. These solutions introduce a correction factor that depends on Δx and that can be applied to Equation (7) if it is solved directly using a pocket calculator and a given Δx.

With values of h_R at each Δx step obtained from topographic or bathymetric maps of the deglaciated landscape, and values of r obtained from Equations (10) and (11) for specified times of glacial advance or retreat, only τ_0 must be specified at each Δx step in Equation (7) in order to reconstruct ice elevations along flowlines of former ice sheets. Values of τ_0 depend on ice velocity, and on how frozen and thawed areas are distributed over the bed. Since τ_0 increases with ice velocity and bed traction, τ_0 is nil beneath ice divides where ice is barely moving and when the ice fraction in subglacial permafrost melts to produce water-saturated muck at the bed. If the bed remains frozen, τ_0 increases from the ice divide to the surface mass-balance equilibrium line because ice velocity must increase in order to transport ice accumulating on the ice-sheet surface. If sheet flow continues to the ice margin, to will increase in the accumulation zone and decrease in the ablation zone, because ice velocity increases and then decreases as ice is gained by accumulation and then lost by ablation. If sheet flow becomes stream flow toward the ice margin, to decreases because ice streams flow over a low-traction bed.

Theoretical variations of τ_0 for sheet flow along an ice flowline have been derived for variable accumulation and ablation rates, variable convergence and divergence of flow, and variable frozen and thawed basal conditions along the flowline (Hughes, 1985). Using accumulation and ablation rates for marine ice domes on the Eurasian Arctic continental shelf specified by Hughes (1985), and using the glacial geology in Figure 3 to specify convergence or divergence of flow and frozen or thawed basal conditions, these theoretical to values can be calculated and used to compute flowline elevation profiles in Equation (7) for sheet flow.

For stream flow along length L_S of a flowline of length L, the counterpart of Equation (7), using an improved version of the analysis by Hughes (1992a), is:

$$h_{i+1} = h_i + \left[\left(1-\frac{\rho_I}{\rho_W}\right)\left(\frac{P_W}{P_I}\right)^2\right]\left[\frac{\dot{a}(h-h_R)_i - (h-h_R)_i^2 (R_{xx}^{*n-1}/A^n)_i (\sigma_{xx}')_i^n}{ax + h_0 u_0}\right]\Delta x$$
$$+ \left[\frac{2}{\rho_I g_z}\left(\frac{\Delta\sigma_{xx}'}{\Delta x}\right)_i + \frac{(\tau_0)_i}{\rho_1 g_z (h-h_R)_i} + \frac{2(\tau_s)_i}{\rho_I g_z W_i}\right]\Delta x \tag{14}$$

where a is the ice accumulation rate, h_0 and u_0 are ice thickness and velocity (u_0 is negative for x positive upstream) at the foot of the ice stream, w is the width of the ice stream, R_{xx}^* represents the stress field, σ_{xx}' is the longitudinal deviator stress, $\Delta\sigma_{xx}'/\Delta x$ is longitudinal deviator stress gradient, to is the basal shear stress, τ_0 is the side shear stress, A and n are the hardness parameter and the viscoplastic parameter in the Nye (1953) flow law of ice, σ_{xx}' is given by:

$$\sigma_{xx}' = \frac{\rho_I g_z (h-h_R)}{4}\left(1-\frac{\rho_I}{\rho_W}\right)\left(\frac{P_W}{P_I}\right)^2 \tag{15}$$

τ_0 is given by:

$$\tau_0 = \tau_v \left(1-\frac{P_W}{P_I}\right)^{\frac{4m}{2m+1}} \tag{16}$$

τ_s is given by:

$$\tau_s = \tau_v \left(\frac{P_W}{P_I}\right)^{\frac{4m}{2m+1}}$$

(17)

ρ_I is ice density, ρ_W is water density, P_I is basal ice pressure, P_W is basal water pressure, m is the viscoplastic parameter in the Weertman (1957) sliding law of ice, modified to include sliding on soft water-soaked sediments or till, and τ_v is the viscoplastic yield stress of ice, defined by Reeh (1982) as:

$$\tau_v = [1/4\,(n+2)\,\rho_I g_z \bar{a} A^n]^{\frac{1}{n+1}}$$

(18)

Equations (14) and (15) are results of the mass balance and the force balance. Equation (16) assumes that bedrock bumps, which control the sliding velocity for sheet flow over bedrock, become progressively drowned by basal meltwater or blanketed by easily deformed till. Equation (17) assumes that the decrease in bed traction along an ice stream causes a proportional increase in side traction (Whillans and van der Veen, 1994). A solution for these equations is obtained by assuming the following variation of P_W/P_I along normalized length x/L_S of an ice stream having length L_S:

$$\frac{P_W}{P_I} = \frac{\rho_I g_z h_W}{\rho_I g_z h_I} \approx \left(1 - \frac{x}{L_S}\right)^c$$

(19)

where h_W is the height to which P_W would raise basal water in an imaginary borehole through ice of thickness h_I, and $0 < c < \infty$ represents the spectrum of basal buoyancy along length L_S of stream flow that converts sheet flow ($c = \infty$) to shelf flow ($c = 0$), with $x = L_S$ at the head and $x = 0$ at the foot of the ice stream. For active ice streams, $0 < c < 1$. For inactive ice streams, $1 < c \ll \infty$. The foot of an ice stream is the grounding line of an ice shelf floating in deep water, a calving ice wall grounded in shallow water, or the head of an ice lobe grounded on dry land.

In applying Equation (14) along flowlines determined by the glacial geology in Figure 3, the $\Delta\sigma_{xx}'/\Delta x$ term can be ignored because, except near the grounding line, it is small compared to the other terms when σ_{xx}' is given by Equations (15) and (19), the ts term can be ignored except in the fjords of Norway and Svalbard, where $(h - h_R)_i$ is not insignificant compared to w_i, $R_{xx'} \approx 1$ if w_i does not vary greatly along L_S, $\tau_v \approx 100$ kPa for viscoplastic yielding in shear, L_S for active ice streams is the length of an interisland channel or a submarine trough formerly occupied by an ice stream, c is chosen to give the same elevation at the ice divide for flowlines down opposite flanks of the ice divide, and u_0 is obtained from the mass flux of ice having thickness h_0 and width w_0 at $x = 0$, as specified by the mass balance for ice converging on the ice stream.

The glacial geology in Figure 3, and the ice-sheet reconstructions in Figures 4 and 5 that are based upon it, are added to the map of the Arctic Region, sheet 14 of the world 1:5,000,000 series of topographic and bathymetric maps produced by the American Geographical Society. The topography and bathymetry were used to specify h_R in Equations (7) and (14).

After sea ice grounds on frozen polar continental shelves, continued snow precipitation causes the grounded sea ice to dome. The bed will remain frozen until the ice-dome thickness is (Robin, 1955):

$$h_I = (T_S - T_M)\,\frac{\sqrt{2}\,K(a h_I/k)^{1/2}}{\sqrt{\pi}\,Q_G\,erf(a h_I/k)^{1/2}}$$

(20)

where T_S is the mean annual surface air temperature and T_M is the basal melting temperature, a is the surface accumulation rate, Q_G is the geothermal heat flux, and h_I is ice thickness, all at the ice divide, K is the thermal conductivity of ice, k is the thermal diffusivity of ice, $(a\,h_I/k)$ is the dimensionless Peclet number, and $erf(a\,h_I/k)$ are error functions tabulated by Abramowitz and Stegun (1965). A dry adiabatic lapse rate of - 1°C

per +100 m in ice elevation was used to compute T_S along the ice divide from a mean sea-surface temperature that was 10°C colder than at the present day.

Figure 4 presents a reconstruction of ice sheets over a frozen bed after 20,000 years of ice accumulation, so r in Equation (10) is calculated for t = 20 ka and t_0 = 5 ka. This is the cold hemicycle of the 41,000 a cycle for tilt of Earth's rotation axis, which controls insolation variations at high latitudes. Marine ice margins are taken at the 200 m bathymetric contour, where ice either calves or becomes afloat, and h_I is calculated from Equation (12) for i = 0 in Equation (7). For terrestrial and lacustrine ice margins, h_I = 100 m at i = 0 is assumed, and ablation is primarily by calving from ice walls. If an ice wall of height h_I neither advances nor retreats, the calving flux must then balance mean accumulation rate along flowline length L from the ice divide to the ice wall such that the calving rate is:

$$u_c = \bar{a}\,(L/h_I) \tag{21}$$

According to calving theory, u_c is given by (Hughes, 1992):

$$u_c = \frac{3\,\rho_I g_z h_I^2 \theta}{\eta_v (c/h_I)^2}\left(1 - \frac{\rho_W h_W}{\rho_I h_I}\right) \tag{22}$$

where η_v is the viscoplastic viscosity of ice, θ is the angle at which the ice wall overhangs from vertical, ρ_W is water density, h_W is water depth, c is the spacing between transverse crevasses behind the calving ice wall, and c/h_I is the calving ratio. From observations of calving for present-day tidewater glaciers:

$$c/h_I \approx 0.40 - 0.35\,(\rho_W\, h_W/\rho_I H_I) \tag{23}$$

In the absence of ice melting, ice calving frequently occurs when $\theta \approx 18°$. The relationship between ice viscosity and ice temperature is provided by Paterson (1981, Table 3.3 and Figure 3.7). At the ice wall, θ_v = 8 x 1013 kg m^{-1} s^{-1} if T = - 10°C is taken. Equations (21) through (23) give:

$$L = \frac{3\,\rho_I g_z h_I^3 \theta\,[1 - \rho_W\, h_W\,/\rho_I h_I]}{\bar{a}\;\eta_v\,[0.40 - 0.35\,(\rho_W\, h_W\,/\rho_I h_I)]} \tag{24}$$

Equation (7) gives $h = h_I + h_R$, with h_I = 100 m at i = 0 used in Equation (24) to calculate L for specified values of h_W/h_I at the ice wall, h_I at $i = L/\Delta x$ is given by Equation (20) for specified values of T_S and Q_G at the ice divide, and h_R is given by topographic and bathymetric maps. The h_I values at i = 0 and $i = L/\Delta x$ determine h_W/h_I for a given L.

A frozen bed beneath the ice divide of a marine ice sheet consists of ice-cemented marine sediments. Therefore, when Equation (20) is satisfied so the bed thaws, the marine sediments will become a slurry that substantially lowers bed traction. The ice divide will lower until basal heat is conducted to the surface rapidly enough to refreeze the bed, thereby restoring basal traction and halting gravitational collapse of the marine ice sheet. The critical ice thickness needed to refreeze the bed beneath the ice divide has been computed by MacAyeal (1993a, 1993b). This ice thickness will be stable if the new values of h_I, T_S, and a at the lowered ice divide satisfy Equation (20). In general, this will not be the case, so the bed will refreeze and ice will thicken until Equation (20) is satisfied at the ice divide for the old values of h_I, T_S, and á.

As the ice divide lowers, ice is evacuated primarily by ice streams, which are fast currents of ice that develop near the ice margin. Ice streams tend to follow interisland channels floored by wet marine sediments along seaward ice margins, and river valleys floored by wet fluvial or lacustrine sediments along landward ice margins. Ice converging at the heads of ice streams generated frictional heat at the bed. This heat causes the frozen-thawed boundary at the heads of ice streams to retreat toward ice divides, where the bed is also thawed. This allows ice streams to lengthen toward ice divides, and gravitational collapse is most rapid when the thawed bed is continuous from the ice divide to the ice margin. Frictional heat is generated at rate $\tau_0\,\epsilon_0$ per unit volume, where ϵ_0 is the

strain rate 6in basal ice. Both τ_0 and ϵ_0 are greatest when the bed is frozen at the head of ice streams, so τ_0 ϵ_0 drives retreat of the basal frozen-thawed boundary. Thawing melts the ice fraction of ice-cemented permafrost, after which τ_0 decreases rapidly because water-soaked basal sediments provide little traction to resist motion of the overlying ice.

Ice-sheet areas and elevations reconstructed over a frozen bed in Figure 4 are redistributed as shown in Figure 5 when the bed becomes thawed. Redistribution of ice is a result of partial gravitational collapse of ice divides and rapid advance of ice margins. This is accompanied by a moderate increase of ice volume, because lowering the ice divide allows convective storm systems to cross more of the ice sheet, thereby increasing accumulation rates, and advancing the ice margin increases the area over which increased precipitation occurs. Southward advance of the marine ice sheet across the Bering Sea continental shelf of central Beringia depresses the snowline of mountain glaciation in eastern Beringia (Alaska) and western Beringia (Siberia), so these glaciers advance as well and they may merge with the marine ice sheet. This allows the ice sheet to cross central Beringia and to calve directly into the Pacific Ocean, thereby preventing faunal and floral migrations across the Beringian land bridge (Hughes and Hughes, 1994).

RETREATING MARINE ICE SHEETS

Low ice elevations and slopes along southern margins of the ice sheet in Figure 5 allow major advances and retreats of this ice margin for minor lowerings or raisings of snowline elevation and slope. The sensitivity to the snowline slope along southern margins of Northern Hemisphere ice sheets was analyzed by Weertman (1961) for a north-south cross-section, using a generalized flow or sliding law that links mass-balance ice velocity u to basal shear stress τ_0:

$$u = C\tau_0^2 \tag{25}$$

where C is a constant evaluated by using Equation (25) to produce a theoretical ice elevation profile along a flowline that matches the known flowline profiles of present-day ice sheets.

When the snowline slope approaches a critical value, of order 10^{-3}, and the ice-sheet slope along the southern margin is steep, as in Figure 4, Weertman (1961) found that height h_L of the ice divide was:

$$h_L \approx (5/3\, C^{1/2} \rho_I g_z)\ (\bar{a}''/s^3)^{1/2} (\bar{a}''/\bar{a}')^{3/5} (1 + \bar{a}''/\bar{a}')^{2/5} \tag{26}$$

where the snowline slope is s and average rates of ice accumulation and ablation are $\bar{a}''$ and $\bar{a}'$, respectively. In addition, length L of the flowline from the ice divide to the ice margin is:

$$L \approx (5/3\, C^{1/2} \rho_I\ g_z)\ (\bar{a}''^3/\bar{a}'^2 s^5)^{1/2} (1 + \bar{a}''/\bar{a}') \tag{27}$$

Note that increasing accumulation rate $\bar{a}''$ or decreasing ablation rate $\bar{a}'$ raises h_L in Equation (26) and lengthens L in Equation (27), and vice versa. Therefore, changing $\bar{a}''$ and $\bar{a}'$ allows the ice sheet to approach a new equilibrium profile. This is the condition for a stable ice sheet.

When snowline slope s is below a critical value, approaching zero, and the ice-sheet slope along the southern margin is low, as in Figure 5, Weertman (1961) found that the height of the ice divide was:

$$h_L \approx h_E (1 + \bar{a}'/\bar{a}'')^{2/5} \tag{28}$$

where h_E is the height of the surface equilibrium line. In addition, flowline length L was:

$$L \approx (3\, C^{1/2} \rho_I g_z / 5)^{2/3} (h_E^5/\bar{a}')^{1/3} (1 + \bar{a}'/\bar{a}'') \tag{29}$$

Fig. 3. Glacial geology and morphology on the Arctic continental shelf, mainland, and offshore islands of Eurasia. From Grosswald and Hughes (in press). Topographic and bathymetric contours are in hundreds of meters.

Note that increasing accumulation rate $\bar{a}''$ or decreasing ablation rate $\bar{a}'$ lowers h_L in Equation (28) and shortens L in Equation (29). The ice sheet becomes smaller, causing height h_L to lower to height h_E until the whole ice sheet is in an ablation zone and the ice sheet shrinks until it disappears. This is the condition for an unstable ice sheet. For example, decreasing $\bar{a}''$ or increasing $\bar{a}'$ allows the ice sheet to grow irreversibly by increasing h_L and L.

Along northern margins of the ice sheet in Figure 5, only accumulation exists along flowlines from the ice divide to the ice margins, and advance or retreat of the ice margin is determined by the stability of the grounding line of an ice shelf floating in the Arctic Ocean. As analyzed by Thomas (1977), retreat velocity v_x of the grounding line is:

$$v_x = \frac{\rho_W/\rho_I)\, v_z + (\alpha - \beta)\, u_x - h_I\, \epsilon_{zz} - a}{\alpha - \beta\,(1 - \rho_W/\rho_I)} \qquad (30)$$

where sea level rises at velocity v_z, α is ice surface slope, β is bed slope, u_x is the (negative) vertical creep thinning strain rate, a is the net accumulation (positive) or ablation (negative) rate averaged for both top and bottom ice surfaces, all measured at the grounding line. Note that the grounding line retreats (positive v_x) when sea level rises (positive v_z), the bed slopes downward toward the ice divide (negative β), creep thins the ice (negative ϵ_{zz}), and ablation exceeds accumulation (negative a).

The vertical ice thinning rate at the grounding line, for transverse strain rate ϵ_{yy} much less than longitudinal strain rate ϵ_{xx}, is given by a modified form of Equation (25):

$$\epsilon \approx -\epsilon_{xx} \approx -C[\,(1/4)\,\rho_I\, g_z\, h_I(1 - \rho_I/\rho_W) - \sigma_B]^3 \qquad (31)$$

where σ_B is the buttressing stress provided by a relatively immobile ice shelf that is nearly land-locked in the Arctic Ocean. Therefore $\sigma_B = 0$ when the ice shelf disintegrates.

If the ice-shelf grounding line lies on the continental slope of arctic Eurasia, β will be positive in Equation (30) and will tend to stabilize the grounding line. In this case, the grounding line will not retreat irreversibly until rising sea level v_z, increasing ice ablation rate a, decreasing ice velocity ux, and reduced buttressing stress σ_B allow the grounding line to retreat upslope until it lies on the downsloping bed of the isostatically depressed continental shelf beneath the ice sheet. Then the northern margin of the ice sheet will retreat irreversibly.

COLLAPSING MARINE ICE SHEETS

Marine ice sheets on the Arctic continental shelf of Eurasia can cycle between the frozen bed configuration in Figure 4 and the thawed bed configuration in Figure 5. Cycling is possible if the unstable retreat of southern ice margins that is permitted by a low snowline slope is stabilized by a steepening snowline slope caused by changing insolation or other factors such as changing atmospheric carbon dioxide, and if the unstable retreat of northern ice margins is stabilized by such factors as rising sea level, decreasing ice velocity, renewed ice-shelf buttressing, and increasing snow accumulation at the ice-shelf grounding line. In addition to these factors, cycling would require the ice sheets to thin enough so that basal heat was conducted to the surface rapidly enough to allow the bed to refreeze. A refrozen bed would then provide the basal traction needed to thicken the ice sheet in Figure 5, even as its margins were retreating, until the ice-sheet thicknesses in Figure 4 were attained, thereby allowing the bed to thaw again.

If the above conditions for cycling are not met, northern and southern margins of the marine ice sheet in Figure 5 would continue to retreat until the ice sheet collapsed. Collapse would be accelerated by two additional factors. First, even as the ice sheet was cycling, so the isostasy ratio r was cycling between the values given by Equations (10) and (11), r would have a trend that increased toward r_0 given by Equation (9) because the ice load would have an increasing trend, even as it was being continually redistributed between the two areal extents shown in Figures 4 and 5. Over time, therefore, the bed would have an increasing downward slope from the ice margin to the ice divide. Second, the increasing bed slope would increase the calving rate from ice walls along the southern ice margin by increasing h_l in Equation (22), and would increase the grounding-line retreat rate along the northern ice margin by making β more negative in Equation (30). Because these additional factors become more important over time, they will eventually tilt the balance between stabilizing and destabilizing

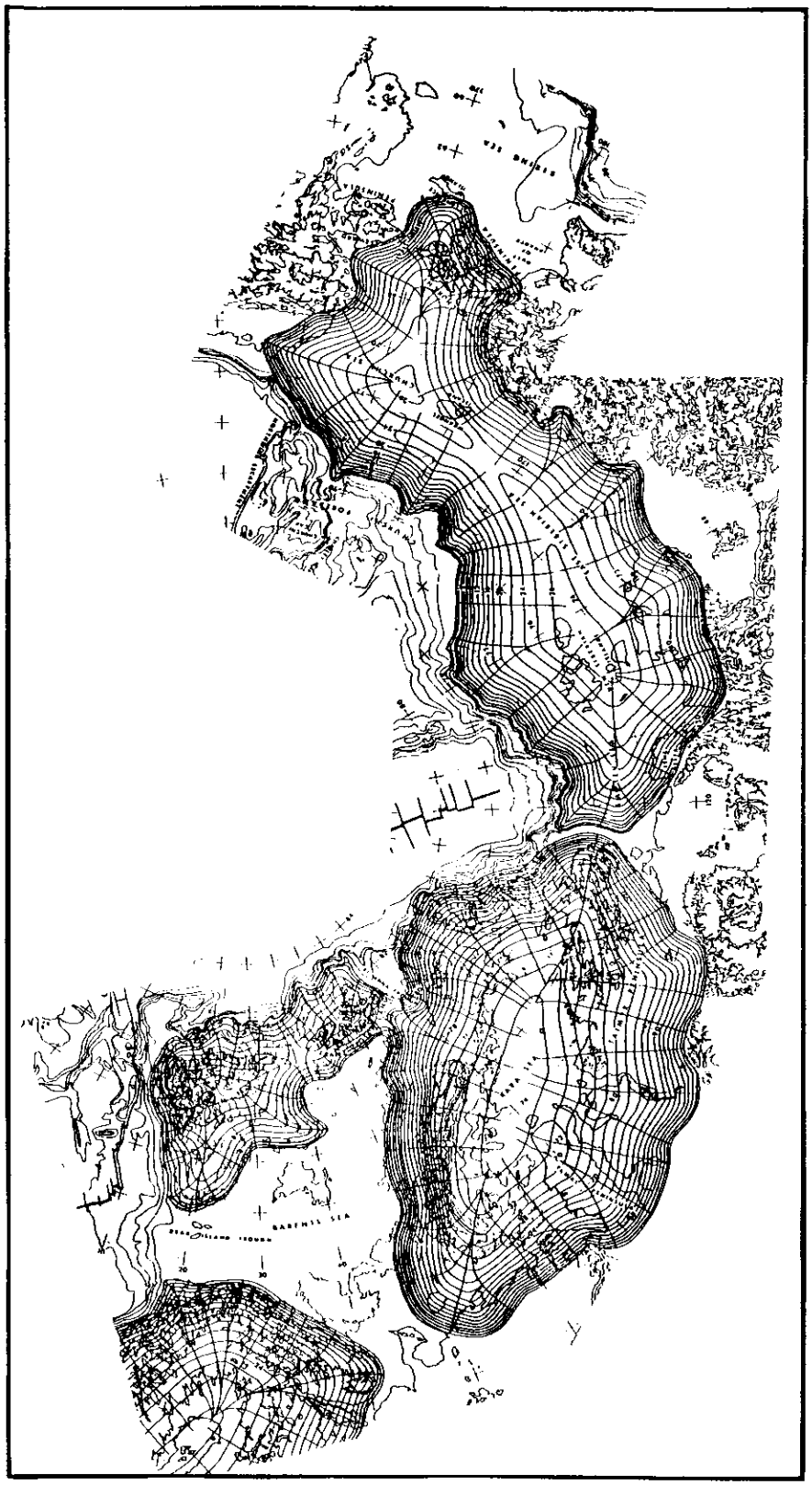

Fig. 4. A numerical reeconstruction of marine ice sheets on a frozen Arctic continental shelf of Eurasia. Ice elevations are contoured at 200 m intervals. Ice margins are constrained by calving along the 200 m bathymetric contour and in water less than 90 m deep along lacustrine margins.

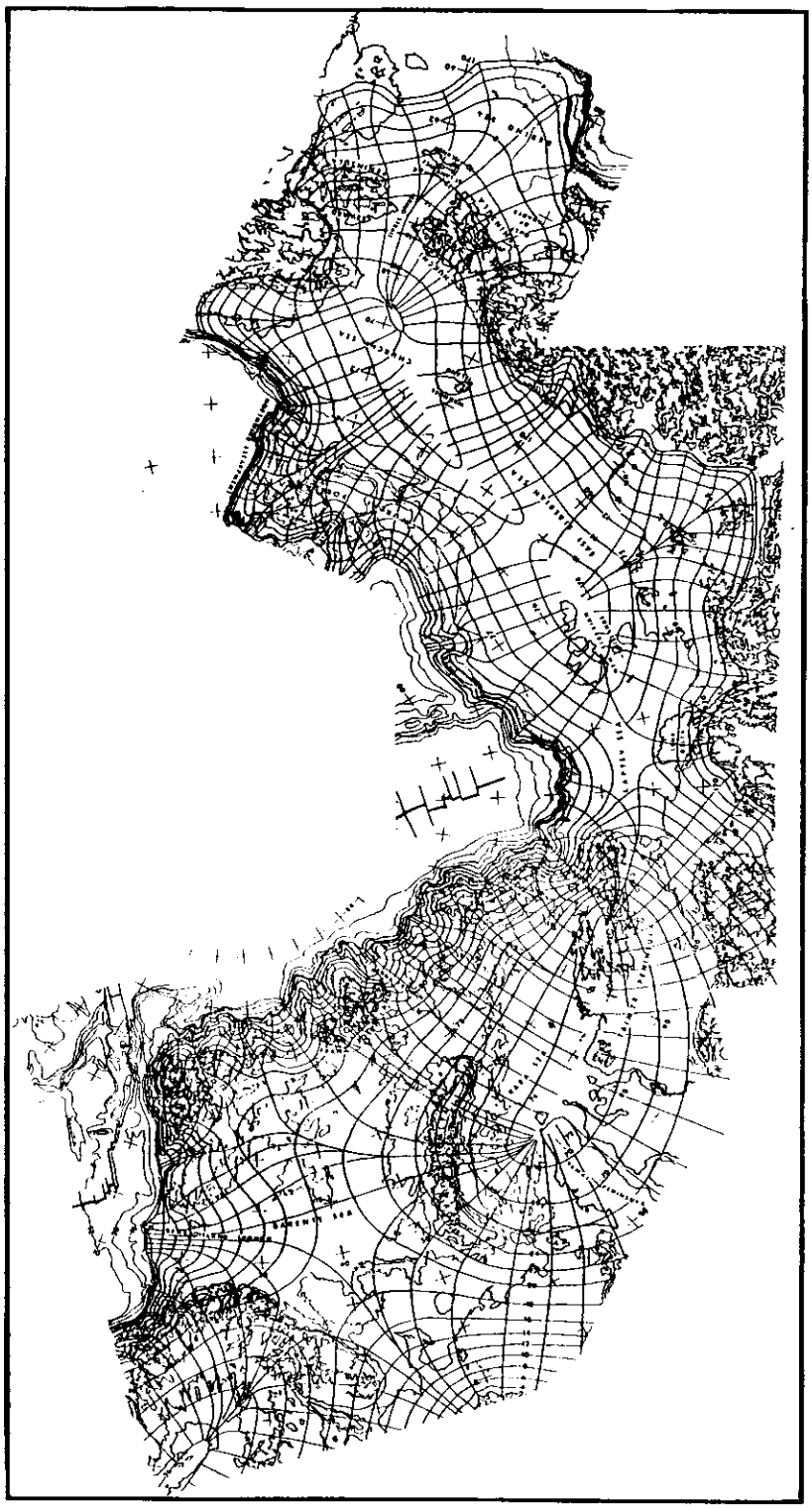

Figure 5. A numerical reconstruction of marine ice sheets on a thawed continental shelf of Eurasia. Ice elevations are contoured at 200-m intervals. Marine ice margins become afloat at the edges of the continental shelf and terrestrial ice margins end as ice lobes supplied by ice streams. In central Beringia, the southern ice margin ends as an ice wall calving into the Pacific Ocean, thereby blocking the Bering landbridge between Siberia and Alaska, and hatchured ice margins denote mergers with mountain glaciation.

factors in the direction of permanent instability. This leads to irreversible retreat of both northern and southern ice-sheet margins, collapse of marine ice sheets, and termination of the glaciation cycle.

DISCUSSION

Glaciological theory presents the possibility that marine ice sheets can nucleate, advance, retreat, and collapse on the broad Arctic continental shelf of Eurasia. Glacial geology and morphology indicate that a marine ice sheet did indeed form and have this history in the western Eurasian Arctic during the last glaciation. Whether this history extended into the eastern Eurasian Arctic, Pleistocene Beringia in particular, is unclear because continuous permafrost limits the glaciological mechanisms that produce glacial geology and morphology, and active cryogenic mechanisms alter or destroy the evidence that was produced. In the absence of such evidence, the prevailing view is that marine ice sheets did not cross central Beringia, at least during the last glacial maximum.

The cycling of marine ice sheets between thick ice over restricted frozen beds and thinner ice over a broad thawed bed, respectively depicted in Figures 4 and 5, represents the extreme upper limits of marine glaciation in Arctic Eurasia. Any degree of marine glaciation, from none at all to these extreme limits, is possible in theory. One attractive possibility in that the extreme sensitivity of the high Arctic to climatic forcing mechanisms does not provide the time needed to attain the high ice-sheet elevations reconstructed in Figure 4. In this case, the bed would not thaw beneath the ice divide and the only mechanism for partial gravitational collapse would be frictional heating of basal ice converging at the heads of ice streams. A thawed bed would exist only beneath ice streams, and the thawed front would extend toward the ice divide only to the extent that ice streams could lengthen toward the ice divide. Therefore, most of the bed would remain frozen, gravitational collapse would be limited to ice streams, and advance of ice margins would be limited to floating ice tongues along northern margins and grounded ice lobes along southern margins, both fed by ice streams.

A program of field research can be designed to explore possible histories of marine glaciation in Pleistocene Beringia. Coring through Pleistocene sediments on the floor of the Chukchi Sea and the Bering Sea is necessary to see if marine, glacial, lacustrine, fluvial, and eolian sequences exist and can be dated. A systematic gravity survey is needed to map the pattern of negative gravity anomalies that would be produced by a marine ice sheet, since fast ice may prevent the wave action needed to produce beaches during glacioisostatic rebound and extensive coastal erosion may destroy beaches that were produced. Surficial dating of cosmogenic nuclides should be employed on bedrock at various elevations along the coastal mainland and on offshore islands, whether or not physical evidence of glaciation exists, to determine when these areas may have been under an ice sheet. More subtly, a shift in mindset is needed that is open to seeking and identifying physical evidence for glaciation by marine ice sheets in environments where permafrost limits the glaciological mechanisms and active cryogenic processes destroy, mask, or alter the evidence that might exist. Examples of such evidence are glacio-marine depositional fans on continental slopes beyond submarine troughs that may have been occupied by ice streams, and lineations associated with a pattern of elongated or beaded lakes along the northern coastal plain of present-day Beringia and which are consistent with ice spreading from a marine ice dome in the Chukchi Sea.

ACKNOWLEDGEMENTS

Many people shaped ideas presented here. In particular, I thank Mikhail Grosswald, Beverly Hughes, Julie Brigham-Greette, Thomas Hamilton, Peter Lea, Stephen Roof, Patricia Heiser, David Hopkins, and David Carter, most of whom made me aware of opposing views. This is an EPSCoR publication.

REFERENCES

Abramowitz, M., and Stegun, I.A., 1965. Handbook of mathematical functions. - New York: Dover.

Ackerman, R.E., 1988. Settlements and sea mammal hunting in the Bering-Chukchi Sea region. - Arctic Anthropology 25(1): 52-79.

Bigl, S.R., 1984. Permafrost, seasonally frozen ground, snow cover and vegetation in the USSR (84-36). - US Army Corps of Engineers (Cold Regions Res. and Engineering Laboratory).

Biryukov, V.Y., Faustova, M.A., Kaplin, P.A., Parlidis, Y.A., Romanova, E.A., and Velichko, A.A., 1988. The paleogeography of arctic shelf and coastal zone of Eurasia at the time of the last glaciation (18,000 B.P.). -- Palaeogeogr., Palaeoclim., Palaeoecol. 68 (2-4): 117-126.

Crary, A.P., 1960. Arctic ice island and ice shelf studies: Part 2. - Arctic 13: 32-50.

Denton, G.H., and Hughes, T.J. (Eds.), 1981. The Last Great Ice Sheets. - N.Y.: Wiley-Interscience.

Gavrilova, M.K., 1981. Recent climate and permafrost on continents. - N-k: Nauka. 270 p. (in Russian).

Grosswald, M.G., and Hughes, T., 1994. Paleoglaciology's Grand Unsolved Problem. - J. Glaciol. In press.
Guthrie, R.D., 1990. Frozen Fauna of the Mammoth Steppe: The Story of Blue Babe. - Chicago: The Univ. of Chicago Press. 321 p.
Hamilton, T.D., 1991. Late Cenozoic glaciation of Alaska. - In: G. Plafker and H. C. Berg (Eds.), The Geology of Alaska (G-1. Chapter 32). Geol. Soc. of America.
Hopkins, D.M., 1972. The paleogeography and climatic history of Beringia during late Cenozoic time. - Inter-Nord 12: 121-150.
Hopkins, D.M., 1982. Aspects of the Paleogeography of Beringia during the Late Pleistocene. - In: D. M. Hopkins, J. Matthews, Jr., C. E. Schweger, and S. B. Young (Eds.) The Paleoecology of Beringia: 3-28.
Hughes, B.A., and Hughes, T.J., 1994. Transgressions: Rethinking Beringian glaciation. - Palaeogeogr., Palaeoclim., Palaeoecol. 110 (3-4): 275-294.
Hughes, T., 1987. The marine ice transgression hypothesis. - Geografiska Ann. 69A (2): 237-250.
Hughes, T., 1992a. On the pulling power of ice streams. - J. Glaciol. 38 (128): 125-151.
Hughes, T., 1992b. Theoretical calving rates from glaciers along ice walls grounded - In: water of variable depths. - J.of Glaciology, 38 (129): 282-294.
Hughes, T.J., 1985. The Great Cenozoic Ice Sheet. - Palaeogeogr., Palaeoclim., Palaeoecol. 50: 9-43.
MacAyeal, D.R., 1993a. Binge/purge oscillations of the Laurentide ice sheet as a cause of the North Atlantic's Heinrich events. - Paleoceagraphy, 8: 775-784.
MacAyeal, D.R., 1993b. A low-order model of the Heinrich-event cycle. - Paleoceanography 8: 767-773.
Nye, J.F., 1953. The flow law of ice from measurements in glacier tunnels, laboratory experiments and the Jungfraufirn borehole experiment. - Proc. Roy. Soc. of London Ser. A 219: 477-489.
Nye, J.F., 1957. The distribution of stress and velocity in glaciers and ice sheets. . - Proc. Roy. Soc. of London Ser. A 239: 113-133.
Paterson, W.S.B., 1981. The Physics of Glaciers. (Second Edition). - Oxford: Pergamon Press. 380 p.
Reeh, N., 1982. A plasticity theory approach to the steady-state shape of a three-dimensional ice sheet. - J. Glaciol. 28 (100): 431-455.
Robin, G.D., 1955. Ice movement and temperature distribution in glaciers and ice sheets. - J. Glaciol. 2 (18): 523-532.
Thomas, R.H., 1977. Calving bay dynamics and ice sheet retreat up the St. Lawrence valley system. - Geograph. Phys. Quaternaire 31 (3-4): 347-356.
Van der Veen, C.J., and Oerlemans, J. (Eds.), 1987. Dynamics of the West Antarctic Ice Sheet. - Proc. of a Workshop held in Utrecht. Dordrecht: D. Reidel.
Weertman, J., 1957. On the sliding of glaciers. - J. Glaciol. 3 (21): 33-38.
Weertman, J., 1961. Stability of ice age ice sheets. - J. of Geoph. Res., 66: 3783-3792.
Wexler, H., 1961. Growth and thermal structure of the deep ice in Byrd Land, Antarctica. - J. Glaciol. 3: 1075-1087.
Whillans, I., and Van der Veen, C.J., 1994. Annals of Glaciology, In press.